Patterns of energy dissipation in three-dimensional face-centred cubic lattices after ion impact

1997 J. Phys.: Condens. Matter 9 5015

(http://iopscience.iop.org/0953-8984/9/23/025)

J. Phys.: Condens. Matter **9** (1997) 5015–5026. Printed in the UK PII: S0953-8984(97)75635-2

Patterns of energy dissipation in three-dimensional face-centred cubic lattices after ion impact

P Guan, D R McKenzie and B A Paithorpe
School of Physics, University of Sydney, Broadway, NSW 2006, Australia

Received 21 June 1996, in final form 10 March 1997

Abstract. Molecular dynamics simulations were performed of the energy dissipation of incident atoms after impact onto a 3D FCC lattice with energies in the range 2–3 keV. The interactions between atoms were described using the Lennard-Jones potential parameterized for copper. The impacting directions were ⟨001⟩ and ⟨101⟩. The results for low energies, of a few electron volts, show that the energy of the impacting atom was dissipated via focused collision sequences (focusons). With increasing energy, cascading bow waves were generated by the focusons, in the close-packed (111) planes only, and carried away the energy of the focusons while, in the high-energy range of a few kiloelectron volts, most of the energy was confined to the lower-index (100) or (110) planes. The structure of these planes was disrupted by secondary focusons generated in these planes, and sputtering occurred when these focusons reach the surface of the substrate. Backward focusons were observed in the low-energy impact case and appeared to be the main reason for the reflection of the impacting ion.

1. Introduction

The problem of energy dissipation after ion impact is a very important topic in the fields of film growth, ion beam mixing, radiation damage and sputtering. The direct experimental observation of phenomena such as collision cascades is severely limited owing to the spatial and temporal limits of resolution of experimental techniques such as electron microscopy and field-ion microscopy. Typically, cascades have dimensions of nanometres and lifetimes of picoseconds. Computer simulation therefore offers the unique ability to examine the process. A considerable amount of work has already been done in this area. Averback's group [1–3] has performed MD simulation of high-energy displacement cascades using the Born–Mayer empirical potential as well as the embedded-atom method (EAM) which use cubic splines to fit the parameters in the pair potential to the atomic density. In their work, the phenomena of replacement collision sequences (RCSs), the thermal spike, melting and cooling and defect creation in the target after kiloelectron volt ion impact were studied in detail. Foreman *et al* [4, 5] carried out similar research using a many-body empirical potential, in the energy range from 60 eV to 2 keV. They found that, for the low-energy cascade, the RCS travels supersonically and there is a well defined wave front within which the atomic are suddenly raised to quite a high temperature. Recently Marks *et al* [6] have carried out a 2D simulation, in which they also found bow waves extending from the energetic head of a focused collision sequence. These waves can travel a distance of more than a 100 Å for a 100 eV impact.

There are, however, many aspects such as the detailed sequence of events taking place during energy dissipation from the impact ion, the detailed pattern of the cascade's evolution

0953-8984/97/235015+12$19.50

and how this pattern is influenced by the energy of the impact ion which have not yet been completely studied. On the other hand, today's powerful computers and visualization techniques facilitate the investigation of such phenomena in large systems on an atomic scale. The purpose of this paper is to give more insight into these things. Our study was divided into three parts by the energy of incident ion:

(1) low-energy impact, in the range 2–20 eV, where we sought to find the energy dissipation patterns during normal film growth;

(2) intermediate-energy impact of 200 eV associated with ion-assisted deposition processes;

(3) high-energy (up to 3 keV) impact, near the lower limit of energies for ion implantation, radiation damage, ion mixing and sputtering.

2. Molecular dynamics simulation

Because of the restriction of computer time, we used different numbers of atoms for each impact energy in our study. For higher energies, a larger system was used because of the larger cascade region. In case (1), a system of size 27 Å × 27 Å × 12 Å with 1280 atoms was used whereas, for (2) and (3), the size was 57 Å × 57 Å × 25 Å with 9216 atoms. In both systems, the lattices are FCC structure with the (001) plane as the impact plane. In the X and Y directions, periodic boundary conditions were employed while, in the Z direction, the first two layers were fixed and the top layer was free. It was assumed that the atoms interacted via the Lennard-Jones 6–12 pair potentials:

$$U_{ij}(r) = 4\varepsilon[(\sigma/r)^{12} - (\sigma/r)^{6}] \tag{1}$$

where ε is the bond energy parameter and σ is the bond length parameter. For computational efficiency, the interaction was truncated at $r = 2.05\sigma$, which means that the interactions up to third-nearest neighbour only were included. Being a central potential, the Lennard-Jones interaction is suitable for describing close-packed systems, such as the noble gases and many metals [6]. The use of this potential enables the interatomic forces to be evaluated with comparatively little computational effort, thus allowing us to include larger numbers of atom in the simulation. Other workers have used more realistic potentials such as embedded-atom potentials [1–3] or combinations between pair potentials, e.g. Morse and Molière potentials [7]. The potentials were parametrized for copper in our study, namely [8]

$$\varepsilon = 0.4096 \text{ eV} \qquad \sigma = 2.338 \text{ Å}. \tag{2}$$

Reduced units were employed in the simulation, by dividing distances by σ and energies by ε and consequently using a basic time unit of $\tau = \sigma(m/\varepsilon)^{1/2} = 0.297$ ps. The integration time steps were 0.001τ for low- and intermediate-energy impacts and $0.000\,01\tau$ for 3 keV impacts.

Impacting copper atoms approached the surface in two directions: ⟨001⟩ and ⟨101⟩. The ⟨001⟩ incident direction simulates normal-incidence film growth while the ⟨101⟩ direction produces focused collision sequences in the substrate as it is a close-packed direction. Before ion impact, both targets were thermostated to 300 K. One difficult problem in realistic simulation of high-energy impacts is the reflection of the focuson when it hits the two fixed bottom layers. The conventional damping method, which stops the movement of the high-energy atoms by applying a damping force of the form $\boldsymbol{F} = -\mu\boldsymbol{V}$, where $\boldsymbol{V}$ is the velocity of the atom, would require too large a value of μ, resulting in unrealistic reflection of energy near the surface. To solve this problem, the method that we used here was to apply a very large damping only to the reflected atoms in the two layers above the fixed

layer, i.e. third and fourth layers in the substrate, which means these atoms were allowed to travel down or sideways but not upwards. In this way, we were able to use a very efficient energy sink to adsorb the energies of the focusons.

3. Results and discussion

Results are presented below for the three energy regimes and the two incident directions studied.

3.1. 2 and 20 eV atom impact

The simulation of copper atoms with incident energies of 2 and 20 eV impacting on a surface atom in the middle area of the substrate has been performed. The behaviour of these incident atoms and their energy dissipation in the substrate are shown in the following two sections.

3.1.1. Behaviour of the incident atoms. Figure 1 shows the kinetic energy and the vertical velocity of the incident atoms as functions of time. In all these cases, there is an acceleration zone near the surface of the substrate, whose depth depends on the cohesive energy between the substrate and the impact atom, and the environment of the impact site. In the case of the 2 eV atom falling in the 'hollow' between the four substrate atoms, the kinetic energy was doubled before the core–core collision. The 'hollow' sites can give another 2 eV to the impact atom before the displacement collision sequence happens. On the other hand, for an impact directly onto a substrate atom, the energy increment of the impacting atom is 40%, about a fifth of the other case, which results from the fact that only one substrate atom accelerates the incoming atom instead of five. In all three cases, adatoms undergo a vibration before settling down. The process is as follows: the first impact loses most of its energy and causes structural distortion of the substrate; then the recovery of the distorted structure will give some energy back to the impact atom. This energy is much higher than that obtained by the recoil from the immediate collision. The latter can only be seen in the V_Z versus time graph in figure 1, the first positive peak (labelled A) which results from the immediate recoiling is much smaller than the second peak which results from the release of the substrate distortion. For the ⟨101⟩, 2 eV impact, the adatom can obtain enough kinetic energy to jump over the nearby hollows. This suggests that the orientation between substrate and ion beam flux is an important factor that can influence the growth of thin films.

3.1.2. Energy dissipation pattern and its influences on the adatoms. Displacement sequences along the close-packed directions were clearly observed after impact. Here we used a cut-off energy of 0.15 eV, which means that any atoms with a kinetic energy higher than 0.2 eV are highlighted in the figures. For normal incidence, there were four focusons travelling along the ⟨101⟩ axes, radiating from the impact site, but the intensities were very small, having only two displacements for each direction for 2 eV impact and five for 20 eV impact. For the ⟨101⟩ impact, only a 2 eV impact was carried out because a 20 eV impact would produce a focuson travelling beyond the edges of the substrate which makes the observation of the backward-travelling focusons impossible. As expected, only one focuson with seven displacements along the impact direction was obtained. This focuson was found to be the main mechanism for the energy loss from the impacting atom. In our case, the addatom was reflected and made a second impact two bond lengths away from the first

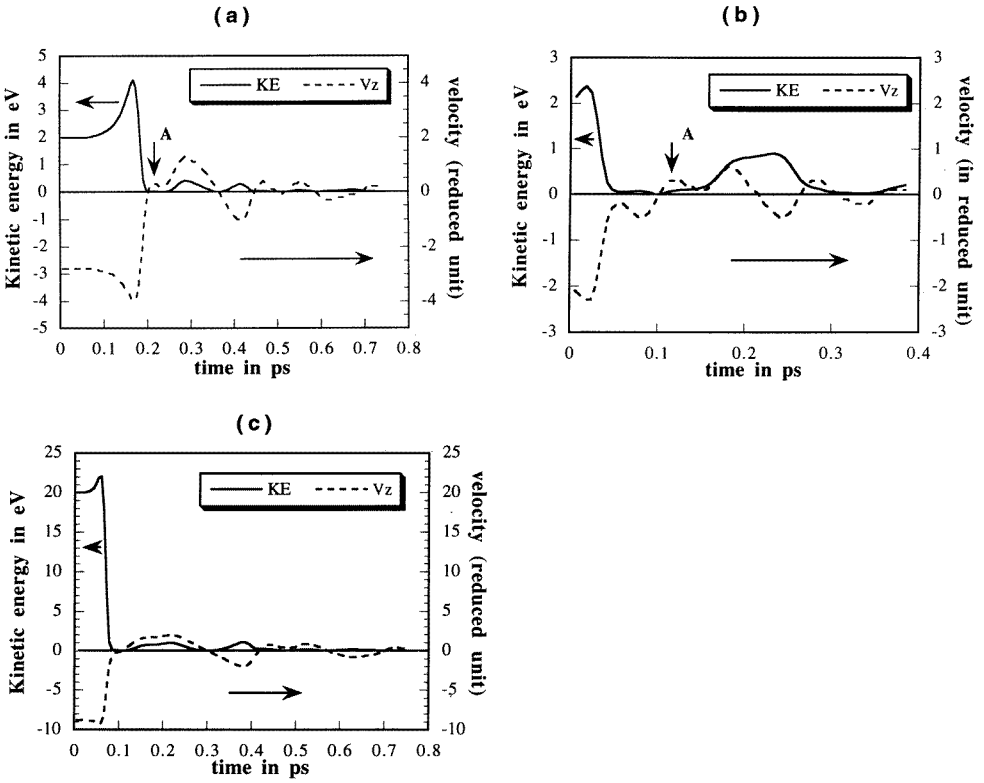

Figure 1. Kinetic energy and vertical velocity of the impact atoms before and after impact: (a) 2 eV normal impact; (b) 2 eV ⟨101⟩ impact; (c) 20 eV normal impact.

impact site and gave the rest of its energy to the atoms there. Finally, the energy was dissipated away from the impact area via lattice vibrations. So, in the low-energy range, the only cascade phenomena observed were focusons. The energy of the focusons was dissipated via lattice vibrations instead of other cascades.

3.2. 200 eV impact

Figure 2(a) shows the energy distribution pattern in one of the (100) planes containing the impact site for a ⟨001⟩ incident atom, in which black dots represent the atoms with kinetic energy higher than 0.15 eV. We can see that energy is transferred along the close-packed ⟨110⟩ directions via focusons. The way that the incident atom loses its energy is by giving energy to all its nearest neighbours and these in turn impart energy to focusons. The way that these focusons lose their energy cannot be viewed in this plane alone. A rapidly attenuated focuson-like sequence is also propagated along the (001) direction beneath the impact site and travels only seven layers into the structure. The focusons can travel significantly farther along the ⟨101⟩ directions but are also attenuated by an energy loss mechanism. To see how these focusons lose their energy, we investigated the energy distribution in the close-packed (111) planes as shown in figures 2(b) and 2(c), which show two adjacent (111) planes. We found that in these planes the distribution pattern for the high-energy atoms was similar to that obtained by Marks *et al* [6] using 100 eVs in a 2D system. In the 2D case, the pattern

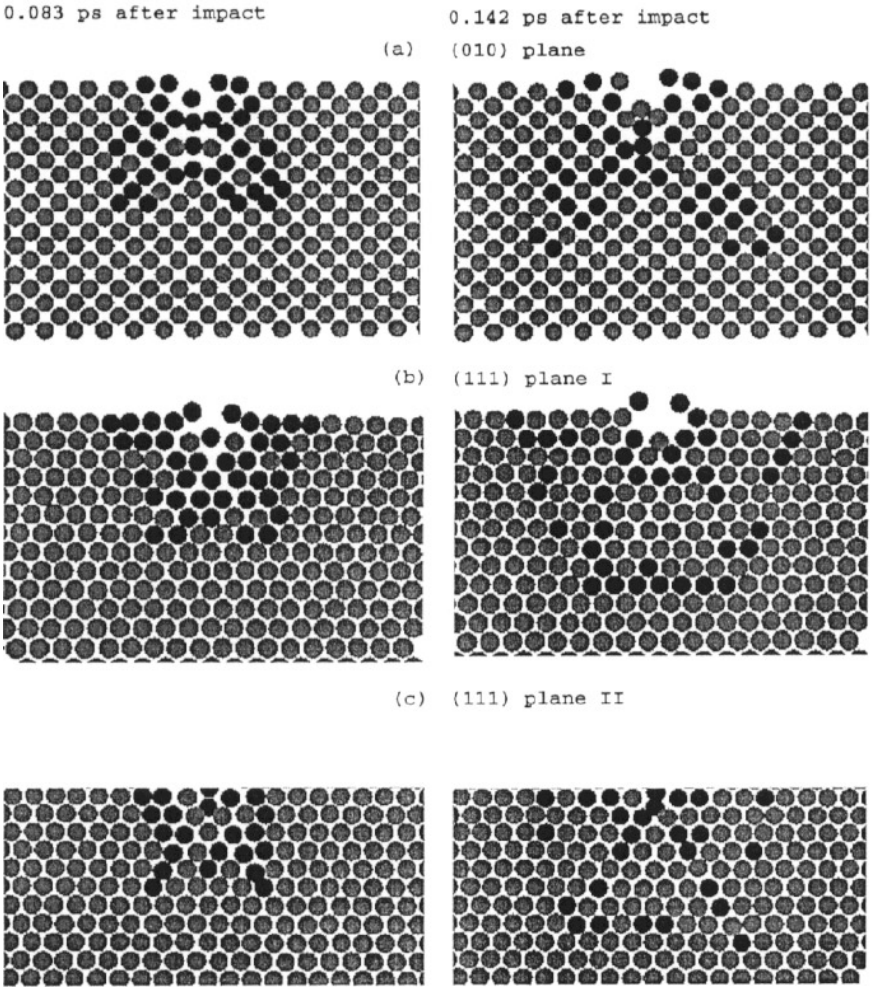

Figure 2. Two snapshots of energy distribution patterns after a 200 eV impact. The black spheres have an energy higher than 0.15 eV. Planes I and II are two adjacent (111) planes with I above II.

is much clearer because energy was confined to a single plane so that no correlation between different layers could occur as in our 3D system. The focusons generated bow waves as in the 2D case, and these are responsible for most of the energy loss from the focuson. We can see that the 2D simulation has similar features to our 3D system. To show in detail how the energy of a focuson is dissipated, the ⟨101⟩ impact was performed. Figure 3 shows the distribution of atoms with kinetic energies higher than 0.15 eV (atoms in the impact line are not included) and figure 4 shows the energy of the focuson (total kinetic energy in the impact line) and the energy contained in the motion of all atoms not taking part in the focuson itself. We can see that most high-energy atoms were excited in the close-packed (111) planes while only a very small fraction appears in the (100) planes. Figure 5 shows the spatial distribution of kinetic energies in one of the close-packed (111) planes being impacted. This result differs from the results of Foreman *et al* [4] who used a many-body potential and a 40 eV impact onto an FCC structure and observed a supersonic shock wave

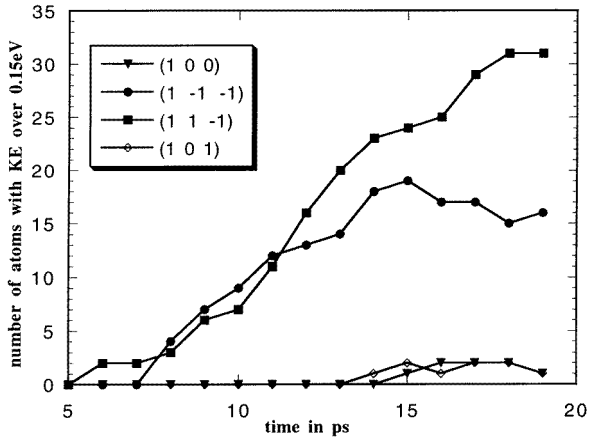

Figure 3. Distribution of higher energy atoms in different planes passed by the focuson.

to be produced in the (100) plane. The bow waves were not observed in our calculation in the (100) planes containing the focuson at this stage perhaps because the energy which the nearby atoms can get from the focuson is small and readily disguised by the thermal energy (only atoms with temperature higher than 1000 K were counted in our case). The results of Foreman *et al* were obtained using a zero background temperature; however, they did not look for the strong bow wave generation in the (111) planes and hence did not observe them. The average velocity of the focuson for 0.0912 ps after impact is 43.17 km s^{-1}, while that of bow waves is around 11.5 km s^{-1} which is much larger than the sound wave velocity of 3.75 km s^{-1} at this point.

3.3. 3 keV impact

Bombardment of materials with kiloelectron volt ions has been of interest in the fields of atomic collisions in solids including radiation damage, sputtering and ion mixing. Although these phenomena have been studied by different workers using different methods, there are still some features of them which have not been studied. Until now, all our simulations take a classical approach which means that ions interact with one another via a potential function and the presence of the electron has not been considered explicitly. This is acceptable when the impact energy is not very high but, for high-energy impacts which result in thermal 'spikes' in the substrate, the effect of electronic stopping cannot be ignored. In this case the equation of motion of the atoms needs to be modified. This is usually done by adding a damping force $\boldsymbol{F}_i$ to each atom in the form

$$\boldsymbol{F}_i = -\mu \boldsymbol{v}_i \tag{3}$$

as has been suggested by other workers [9], where μ can be written as

$$\mu = \alpha m \frac{T_i - T_e}{T_i} \tag{4}$$

where i is the ion index, T_i and T_e are the ion and electron temperatures, respectively, m is the ion mass and α is a constant dependent on both the material and the electron temperature. T_i can be expressed as $T_i = mv^2/3k$ and T_e can be taken as the ambient temperature. For an ambient temperature of 300 K, the product αm is equal to 0.21 in reduced units. Because

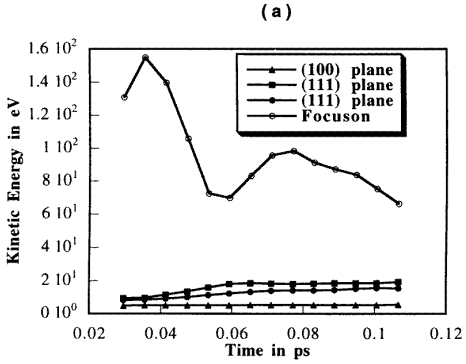

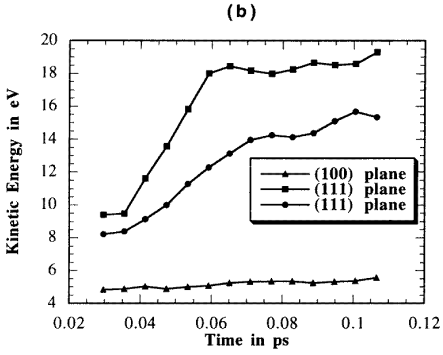

Figure 4. (a) The variation in energy of the focuson and the cascades with time; (b) the energies of cascades in different planes.

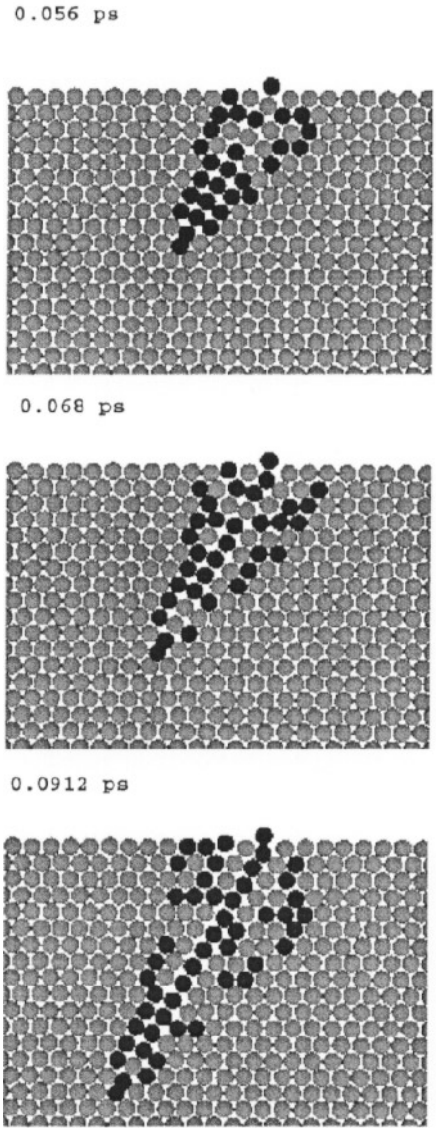

Figure 5. The close-packed plane (a) 0.056 ps, (b) 0.068 ps and (c) 0.0912 ps after a 200 eV ion impact at 45°. The black spheres represent atoms with an energy greater than 0.15 eV.

of the restriction of the small system that we used, this study will be more suitable for the initial stage in the thermal spike formation than for the whole lifetime of thermal spike, which may include the production of self-interstitial atom (SIA) defects. On the other hand, the latter have well been studied by many other workers while the thermal spike has rarely been mentioned. In our study, ⟨001⟩ and ⟨101⟩ impacts were performed.

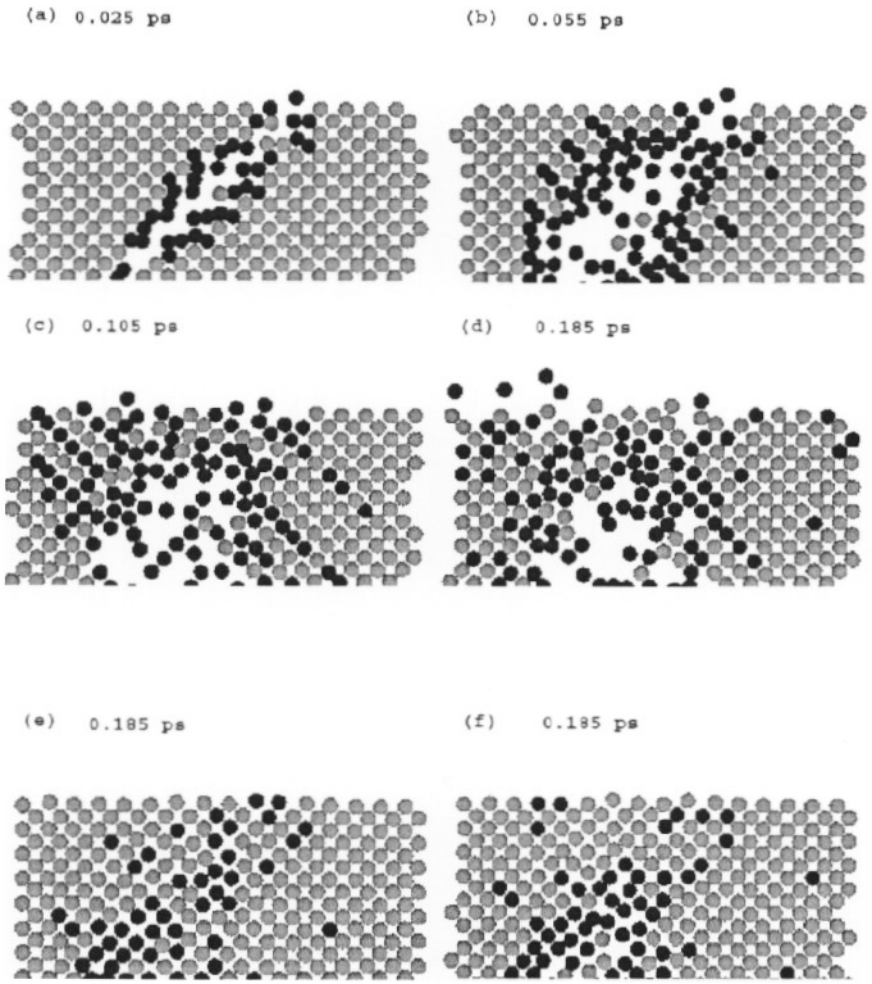

Figure 6. Snapshot of the (100) plane (a) 0.025 ps, (b) 0.055 ps, (c) 0.105 ps and (d) 0.185 ps after a 45° impact with a 3 keV ion. (e), (f) Two neighbouring planes of the above plane.

3.3.1. ⟨001⟩ impact. Figure 6 shows what happened in the (100) plane containing the impact ion. Figures 6(a)–6(d) show the following.

(a) Defocusing was found to occur as reported by Gibson *et al* [10].

(b) This 'defocuson' developed into a secondary focuson on a travelling path perpendicular to the impact direction and atoms are ejected from the core of the cascade, creating a depleted zone.

(c) Energy transferred to surface atoms in the form of focusons causes these atoms to be ejected from the surface, a process generally referred to as sputtering.

(d) It is also found that this process happens only in the plane being directly impacted.

The adjacent planes are not significantly influenced as seen in figures 6(e) and 6(f). Figure 7 shows the kinetic energies of cascades in different planes (here only (100) and (111) planes are compared because no direct collision occurs with the atoms in (101) plane). Contrary to the case of low-energy impact, most of the energy is dissipated through the less

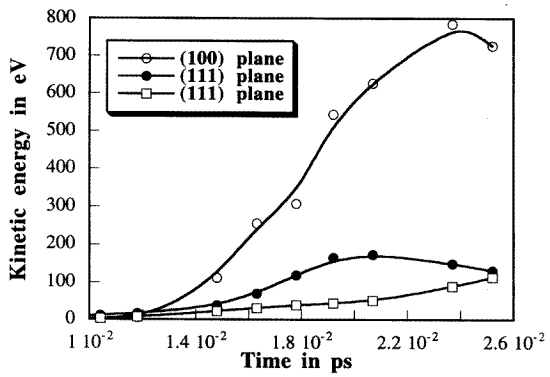

Figure 7. Energy distribution in different planes after a 3 keV ion impact at 45°.

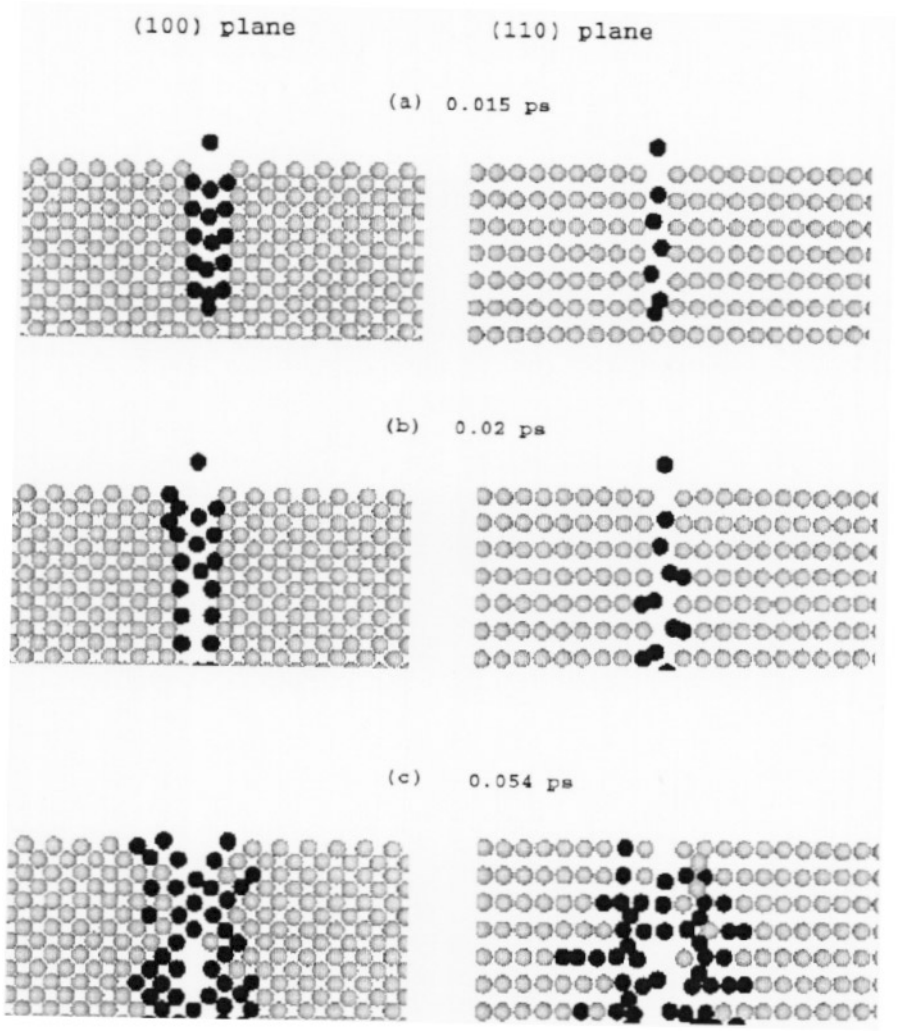

Figure 8. Snapshot of (100) and (110) planes (a) 0.015 ps, (b) 0.02 ps and (c) 0.054 ps after 3 keV impact in the normal direction.

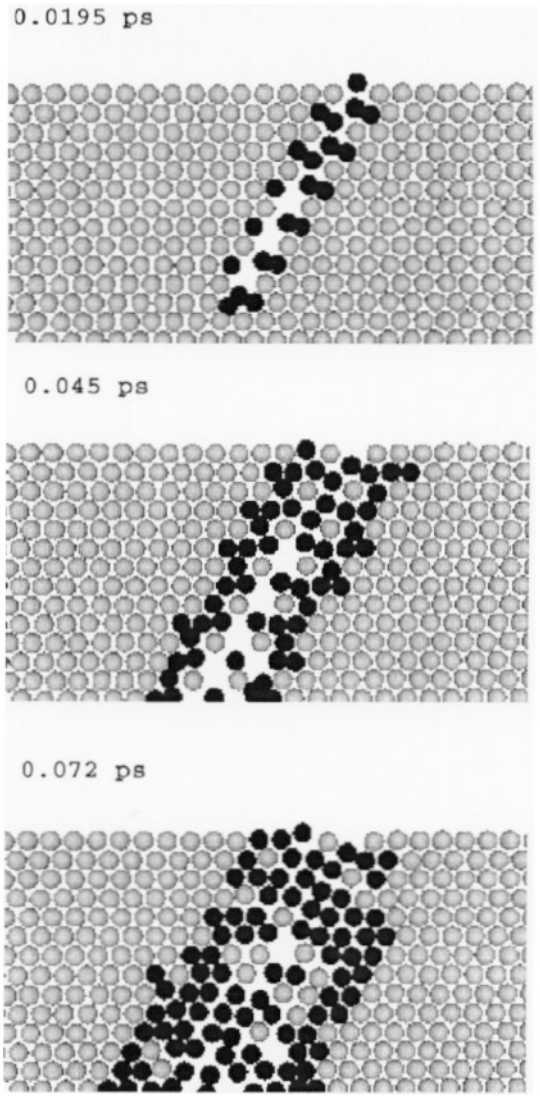

Figure 9. Snapshot of (111) plane after 3 keV impact at 45°.

densely packed planes. Comparing these two cases, we found that, in low-energy impacts, the high-energy atoms in the line of impact were still confined in that line while, in high-energy impacts, these atoms were knocked off the line and moved outwards in the (100) plane carrying a much higher energy. Also, the surface atoms beside the sputtered atoms were not much influenced at the time of sputtering. In fact, the sputtering and production of SIA defects have the same mechanism and arise from RCSs. When the RCS reaches the surface, sputtering will occur along the direction of the RCS. In figure 6(d), we see that two atoms in the same RCS were ejected and sputtered atoms were observed.

3.3.2. ⟨*001*⟩ *impact.* As in ⟨101⟩ impacts, some phenomena for intermediate-energy impacts were not observed when the impacting ion has a high energy. The substrate response in two planes is as follows.

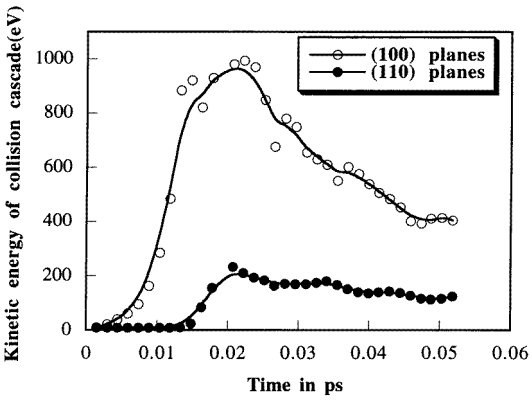

Figure 10. Energy transferred to (100) and (110) planes after 3 keV normal impact.

(a) From the (100) plane, the direction of energy transferral was not as obvious as in the intermediate-energy case where the pattern of energy dissipation is by focusons and bow waves.

(b) In the (111) plane, the characteristic supersonic bow wave patterns were not obtained.

Figure 8 illustrates these results in these two planes along the impact direction. We found that, just after impact, most energy was transferred downwards, forming a tunnel of only the four nearest atoms along the impact line, and no focusons were found in the (100) plane just as in low-energy impact case. On comparison with the ⟨101⟩ impact, the energy dissipation pattern in the (100) plane has similar features to the (111) plane as shown in figure 9: a parallel pattern of cascades along the impact line, with the structure little disturbed except in the impact line where the atoms were knocked off the plane. In the (110) plane we see a similar pattern to the (100) plane for ⟨101⟩ impact (cf figure 6), creating focusons in the ⟨110⟩ direction and distorting the structure afterwards. Figure 10 shows the fraction of energy transferred to the (100) and (110) planes. We can see that in both cases most of the energy is dissipated through (100) planes and it seems that focusons form much more easily in the directions that lie perpendicular to the impact line.

4. Conclusion

We have investigated the energy dissipation pattern in a Cu FCC lattice after ion impacts with different energies. The main conclusions can be summarized as follows.

(1) In low-energy impacts, the energy is dissipated into the target by weak focusons and then lattice vibrations. The backward focusons can cause reflection of the incident ion.

(2) When the impact energy is raised to several hundreds of electron volts, supersonic shock waves are produced in close-packed planes and are the main mechanism for the energy dissipation of the impact ion.

(3) For kiloelectron volt impacts, low-index (100) planes will carry off most energy of the shock waves resulting from the impact instead of the (111) plane as in (2).

From this study, we can see that the energy dissipation pattern of the impact ion depends on the structure of the target and incident direction. This dependence, however, can vary with increase in the incident energy. For better understanding of some of the phenomena, a larger system with a longer simulation time will be necessary.

Acknowledgments

The authors acknowledge financial support by Overseas Postgraduate Research Scholarship and University Postgraduate Research Awards within Sydney University. We wish to thank VisLab at the University of Sydney for access to the Cray supercomputer and extensive visualization resources. We are especially grateful to N A Marks for his help throughout the whole research.

References

[1] Diaz de la Pubia T, Averback R S, Benedek R and King W E 1987 *Phys. Rev. Lett.* **59** 1930
[2] Hsieh H, Diaz de la Rubia T and Averback R S 1989 *Phys. Rev.* B **40** 9986
[3] Averback R S and Ghaly M 1994 *Nucl. Instrum. Methods* B **90** 191
[4] Foreman A J E, English C A and Phythian W J 1992 *Phil. Mag.* A **66** 655
[5] Foreman A J E, Phythian W J and English C A 1992 *Phil. Mag.* A **66** 671
[6] Marks N A, McKenzie D R and Paithorpe B A 1994 *J. Phys.: Condens. Matter* **6** 7833
[7] Mueller K H 1987 *J. Appl. Phys.* **61** 2516
[8] Halicioglu T and Pound G M 1975 *Phys. Status Solidi* **30** 619
[9] Finnis M W, Agnew P and Foreman A J E 1991 *Phys. Rev.* B **44** 567
[10] Gibson J B, Goland A N, Milgram M and Vineyard G H 1960 *Phys. Rev.* **120** 1229